Turn On of a Ruthenium(II) Photocatalyst by DNA-Templated Ligation

Anzola, Marcello; Winssinger, Nicolas

How to cite

ANZOLA, Marcello, WINSSINGER, Nicolas. Turn On of a Ruthenium(II) Photocatalyst by DNA-Templated Ligation. In: Chemistry - A European Journal, 2019, vol. 25, n° 1, p. 334–342. doi: 10.1002/chem.201804283

This publication URL: https://archive-ouverte.unige.ch/unige:112587
Publication DOI: 10.1002/chem.201804283

Turn On of a Ruthenium(II) Photocatalyst by DNA-Templated Ligation

Marcello Anzola and Nicolas Winssinger*

Department of Organic Chemistry, NCCR Chemical Biology, Faculty of Science, University of Geneva, 30 quai Ernest Ansermet, 1211 Geneva, Switzerland.

ABSTRACT: Here, the synthesis of a Ru^{II} photocatalyst by light-directed oligonucleotide-templated ligation reaction is described. The photocatalyst was found to have tremendous potential for signal amplification with >15000 turnovers measured in 9 hours. A templated reaction was used to turn on the activity of this ruthenium(II) photocatalyst in response to a specific DNA sequence. The photocatalysis of the ruthenium(II) complex was harnessed to uncage a new precipitating dye that is highly fluorescent and photostable in the solid state. This reaction was used to discriminate between different DNA analytes based on localization of the precipitate as well as for in cellulo miRNA detection. Finally, a bipyridine ligand functionalized with two different peptide nucleic acid (PNA) sequences was shown to enable template-mediated ligation (turn on of the ruthenium(II) photocatalysis) and recruitment of substrate for templated photocatalysis.

Templated reactions are accelerated by the high effective concentration of reagents achieved in a supramolecular assembly. Oligonucleotides offer a particularly attractive platform for templated reaction based on the fact that affinities of the supramolecular interactions are readily tunable, they can be multiplexed through unique oligonucleotide sequences and have important applications.[1–4] This has stimulated significant efforts in the area, with a growing number of reactions extending the breadth and scope of templated transformations. Prominent examples include nucleophilic reactions,[5–7] olefinations,[8–9] Staudinger reactions,[2, 10–12] conjugate additions,[13] native chemical ligations or acyl transfers,[14–17] and cycloadditions.[18–20] Important applications of these reactions include the synthesis of small molecule libraries, nucleic acid sensing or drug uncaging. The majority of the reactions are designed to bring two reagents, each conjugated to unique oligonucleotides, in proximity upon hybridization to a template (Figure 1). Template turnover requires the exchange of both reagents. Most examples of templated reactions do not surpass 100 turnovers relative to the template. We have shown that the photocatalytic activity of $[Ru(bpy)_3]^{2+}$ type of complexes can be harnessed to reduce different immolative linkers, enabling substrate turnover with only one reagent exchanging on the template. However, these studies clearly point to the fact that substrate turnover is rate limiting.[21–23] Alternatively, a templated reaction could be used to generate an active catalyst. Transition-metal catalysts are capable of high turnover numbers. Thus, a nucleic acid-templated formation of an active transition-metal catalyst from catalytically inactive precursors could be used to convert substrates with high signal amplification overcoming the rate-limiting step of templated reactions (substrate turnover/product inhibition). Surprisingly, this templated reaction format has not received much attention despite some previous achievements in the area. One of the first examples of templated reactions extending beyond questions related to prebiotic chemistry was reported by Sheppard in 2001.[24] In this example, a metallosalen complex was prepared in a DNA templated fashion and shown to be effective in DNA-cleavage reactions. Subsequently, Herrmann demonstrated that a $Pd(PPh_3)_2$ catalyst could be generated from two oligonucleotides coupled to triphenylphosphine that can coordinate to palladium.[25] However, due to competing coordination from nucleobases, the chemistry had to be performed under acidic conditions (pH 5). Tris(bipyridyl)ruthenium(II) complexes are remarkably stable and have enjoyed a renewed interest in the scope of transformations they can promote.[26] Such complexes are currently used in

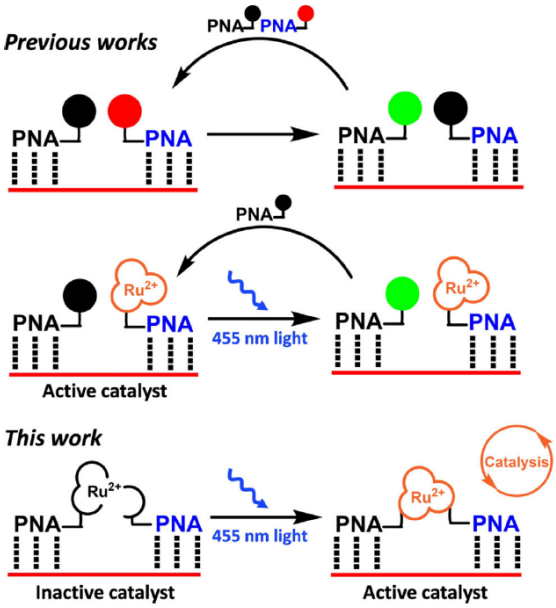

Figure 1. Nucleic acid-templated transformation with: stoichiometric amounts of exchanging reagents (top); active photocatalyst with exchange of a single reagent (middle); formation of the active photocatalyst without exchange of reagents (bottom).

humans for photodynamic therapy[27] and we have shown that ruthenium-photocatalyzed reactions can be performed in cells as well as in living organisms.[21,28] Here, we demonstrate that a surrogate of tris(bipyridine)ruthenium(II) complex can be prepared in a templated fashion, resulting in a turn-on of the ruthenium complex photocatalytic properties (Figure 1).

EXPERIMENTAL SECTION

Preparation of final ruthenium(II) or coumarin derivative. Compound **2** (or **S18** in the Supporting Information) was dissolved in 50 µL of N-methyl-2-pyrrolidone (NMP) to obtain a 0.1M solution (5 equiv to 5 mg of resin loaded at 0.2 $mmolg^{-1}$). TBTA (2 mg, 4 µmol, 4 equiv) was added as a solid. 15 µL of a 0.4M solution of $CuSO_4$ in water (6 equiv) was added, followed by 50 µL of 2M aqueous solution of sodium ascorbate (100 equiv). The yellow solution was transferred onto the resin and reacted overnight. Final compounds were purified by reversed-phase HPLC.

Cleavage from the resin. The N-terminus of the PNAs was capped if needed. The resin was suspended in TFA (200 µL for 5 mg resin) for 1 h. The PNA was then precipitated from diethylether and centrifuged to recover the product as a pellet.

Synthetic templates. DNA sequences were purchased from Eurogentech as solids.

Representative procedure for ligation. Ligation was carried out by mixing DNA and PNAs in PBS 1x buffer with 0.05% Tween 20 and 0.1% formamide (pH 7.4) to a final concentration of 5 mm and a final volume of 100 µL in a 96-well plate (Nunc). The plate was placed at 40 °C and irradiated with a λ=455 nm LED (1 W, 2 cm distance), unless otherwise stated. At different time intervals, luminescence was recorded using a SpectraMax M5 Microplate Reader from Molecular Devices for a 96-well plate at λ_{ex} : 450 nm, λ_{em}: 630 nm.

Beads loading. Streptavidin–agarose resin, high capacity, was purchased from Thermo Scientific. Binding capacity was calculated to be 550 pmol of biotin 4-nitrophenylester μL^{-1} of settled resin, based on the supplier specifications. 10 µL of settled resin was treated with 20 µL of a 9:1 solution of 100 µM biotin (1800 pmol) and 100 µM biotinylated PNA-bpy^3 (200 pmol) by incubating for 1 hour. Beads were washed and resuspended in 200 µL of water.

QPD precipitation on beads. 50 µL of resuspended beads (2.5 µL of settled resin) was added to a 1 mL of 200 nM PNA-Ru (200 pmol) and 1 mL of **DNA 1** at different concentrations in a 35 mm petri dish. The mixture was incubated and shaken for 2 hours in the dark at room temperature. The ligation reaction was performed at 40 °C, shining blue light for 1 hour. After the ligation, sodium ascorbate and **5** were added to a final concentration of 10 mM and 50 µM. Precipitation was elicited by irradiation of the beads with a 488 nm laser, and fluorescence was recorded using a Zeiss LSM710 confocal microscope. λ_{ex}: 730 nm (2P) 20%, λ_{em}: band-pass filter 500–550 nm.

Fluorescence quantification on beads. Confocal images were analyzed and quantified using FIJI software. Ch1 (fluorescence channel) of each image was Z-stacked to its maximum projection. The image was duplicated for thresholding. The beads were highlighted and added to the regions of interest (ROI) manager, and the threshold was set at 20–255. ROIs were combined and treated as a single ROI. Particles of size (µm2) 1-Infinity were analyzed, reporting the analysis to the original image. The reported values of mean grey and area% were multiplied to give the values used for the statistics, based on the assumption that a higher concentration of template should give a brighter and denser precipitate on the beads.

miRNA21 templated ligation. 104 MCF-7 cells were seeded in a 35 mm dish and incubated at 37 °C for 24 hours. Cells were washed three times with Dulbecco's phosphate-buffered saline (DPBS, without magnesium and calcium), then fixed with a 4% PFA solution for 20 minutes at room temperature. Following fixation, cells were washed three times with DPBS and PNA6-Ru and bpy-PNA5 or PNA6-Ru and bpy-PNA3 (100 nM in DPBS) were added to the dish. Cells were incubated at 37 °C for 2 hours, and then washed once with cold DPBS. Ligation was performed through 455 nm irradiation of the dish at 37 °C for 1 hour. The cells were washed again once with cold DPBS, sodium ascorbate (20 mM) and **5** (20 µM) added. After 1 hour incubation at 37 °C, cells were irradiated with blue light for 30 minutes at room temperature. Cells were washed three times with cold DPBS and then imaged using a Zeiss LSM710 with settings λ_{ex}: 730 nm (2P) 20 %, λ_{em}: band-pass filter 500–550 nm.

RESULTS AND DISCUSSION

We had previously used a $[Ru(bpy)_2(phen)]^{2+}$ complex as a substitute for $[Ru(bpy)_3]^{2+}$, based on the fact that the isothiocyanate $[Ru(bpy)_2(phen\text{-}NCS)]^{2+}$ is commercially available and its conjugation to oligonucleotides is straightforward.[21, 23, 28, 29]While there are more examples of photocatalysis in the literature with $[Ru(bpy)_3]^{2+}$ than $[Ru(bpy)_2(phen)]^{2+}$ and its related analogs, both complexes have very close redox potentials and photophysical properties; hence, the well-established photocatalysis of $[Ru(bpy)_3]^{2+}$ can be extrapolated to $[Ru(bpy)_2(phen)]^{2+}$. These complexes are generally prepared from cis-dichlorobis(2,2'-bipyridine)ruthenium(II) by

substitution with the third bidentate ligand (bipyridine or phenanthroline). Although such displacement reactions could be envisioned to be performed in a templated fashion, the high temperatures required (typically performed at >100 °C) seemed excessive in the context of nucleic acid-templated processes. On the other hand, it is known that monodentate ligands on bis(bipyridine)ruthenium complexes can exchange under mild conditions following photoexcitation at 450 nm.[30–31] This ligand exchange has indeed been used to uncage bioactive compounds in animal models.[32] Thus, we reasoned that, although the templated ligation to form the catalyst would be challenging under thermal conditions, it should proceed under 450 nm irradiation at physiological temperatures. We set out to prepare ruthenium(II) complexes **1** and **2** with an alkyne on the phenanthroline for conjugation to peptide nucleic acids sequences (PNA, Scheme 1).

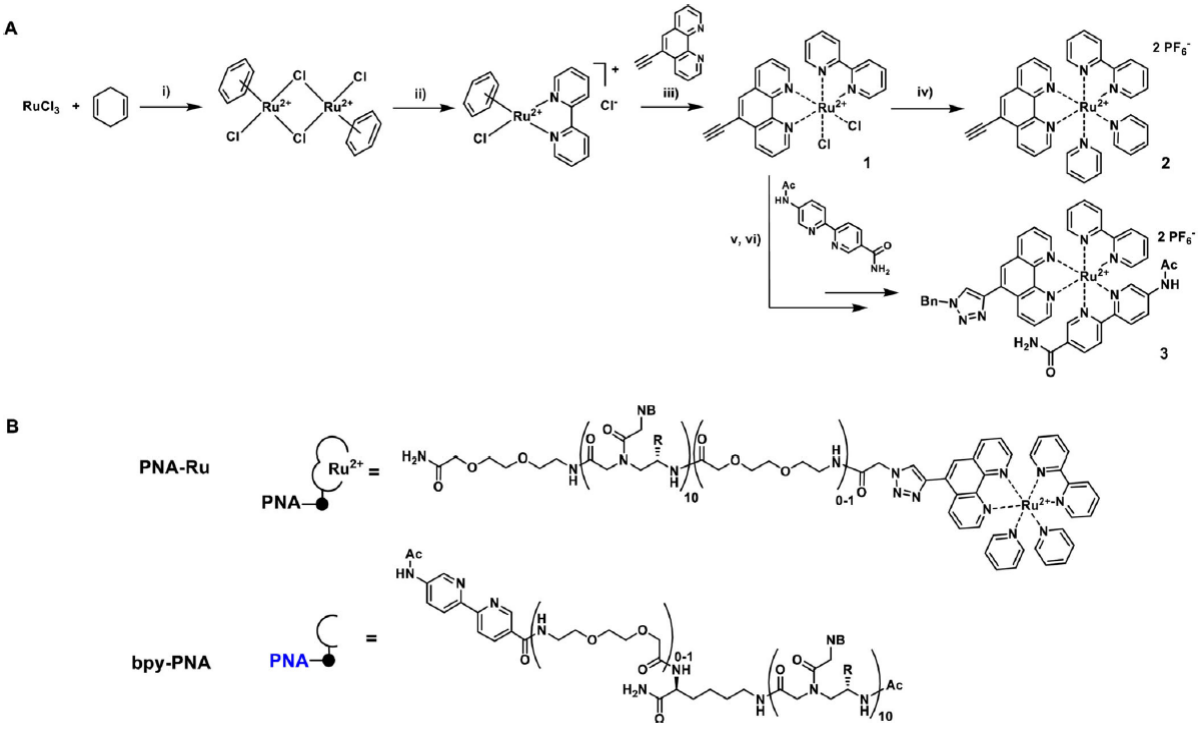

Scheme 1. A) Synthetic route for ruthenium(II) complexes. i) EtOH, microwave irradiation, 130 °C, 4 min; ii) 1 equiv bpy, MeCN, microwave irradiation, 120 °C, 10 min; iii) 1 equiv 5-ethnyl-phenanthroline, DMF, 90 °C, 8 h. iv) excess pyridine, MeOH/H_2O 4:1, 90 °C, 9 h; v) MeOH/H_2O 4:1, 90 °C, 9 h; vi) BnN_3, DMF, CuBr, TBTA, RT, 1 h. B) General structures of the PNA sequences used in the experiments. Black spheres indicate the optional [2-(2-aminoethoxy)ethoxy]acetic acid spacer. R = H, CH_2OH.

The synthesis started with ruthenium trichloride that was reacted with 1,4-cyclohexadiene to obtain $[RuCl_2(\eta\text{-}C_6H_6)]_2$. This complex was engaged in two successive substitution reactions with bipyridine and 5-ethynyl-1,10-phenanthroline (commercially available or readily prepared from phenanthroline in three steps)[33] to afford complex **1**. The two remaining chlorides were further substituted with pyridines to afford complex **2**, which was considered a better starting material for templated reactions based on its stability and the use of related complexes in biological settings.[32] In parallel, we prepared the templated-ligation product **3** by using 5'-acetamido-(2,2'-bipyridine)-5-carboxamide [prepared from 5'-amino-(2,2'-bipyridine)-5-carboxylic acid]. Complex **2** was found to conjugate smoothly to PNAs functionalized with an azide by copper(I)-catalyzed alkyne-azide cycloaddition (CuAAC). The bipyridine-PNA adduct was prepared by standard coupling conditions.

It is known that $[Ru(bpy)_3]^{2+}$ and its analogues can be used as photocatalysts in the reduction of N-alkyl-pyridinium protecting groups with subsequent liberation of a caged functional group (ester, carbonate, carbamate, phenolic ether).[34, 35] Using a pyridinium-caged coumarin,[23] the photocatalytic activity of the precatalyst (complex **1** or **2**) was tested, and compared to the catalyst resulting from ligation (complex **3**). As anticipated, the two precatalysts were found to be catalytically inactive towards the reduction of a caged fluorophore, whereas complex **3** led to coumarin liberation by photocatalytic pyridinium uncaging (Figure 2A, B). We then tested the performance of catalyst **3** at high substrate concentration and low catalyst loading to maximize the turnover number.

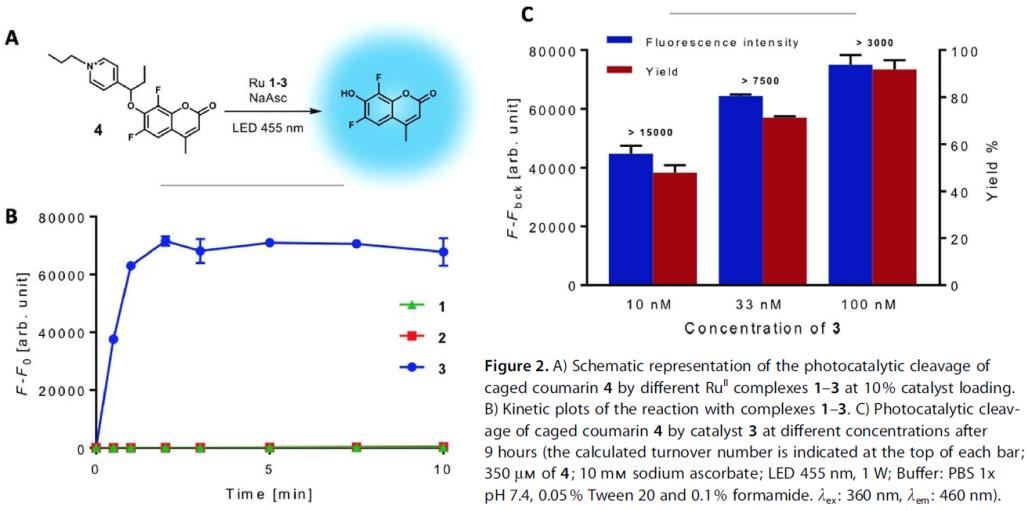

Figure 2. A) Schematic representation of the photocatalytic cleavage of caged coumarin **4** by different Ru^{II} complexes **1**–**3** at 10% catalyst loading. B) Kinetic plots of the reaction with complexes **1**–**3**. C) Photocatalytic cleavage of caged coumarin **4** by catalyst **3** at different concentrations after 9 hours (the calculated turnover number is indicated at the top of each bar; 350 μM of **4**; 10 mM sodium ascorbate; LED 455 nm, 1 W; Buffer: PBS 1x pH 7.4, 0.05% Tween 20 and 0.1% formamide. λ_{ex}: 360 nm, λ_{em}: 460 nm).

The reaction was carried out in deaerated phosphate buffered saline (PBS), to prevent oxygen quenching and take full advantage of the efficiency of the catalyst. Impressively, compound **3** was found to be capable of more than 15 000 turnovers in 9 hours (Figure 2C). Having demonstrated that only the tris-bidentate chelated RuII complex **3** is suitable as a catalyst, we next investigated the light-promoted and templated formation of the catalyst. PNA sequences complementary to the DNA template were prepared according to the previously developed Mtt/Boc-based protection strategy with γ-modified PNA monomers[36] (see Table S1 in the Supporting Information for the full list of sequences and PNA characterization for explicit structures). PNA 10-mers were used because this length is sufficient to generate duplexes with DNA that are suitably long-lived for templated reactions to proceed. As shown in Scheme 1, complex 2 was introduced at the N-terminus of a PNA sequence, whereas the bipyridine ligand was coupled to the C-terminus of another PNA sequence. To discover the most favorable preorganization of the reagents for a ligation, following hybridization, PNAs were prepared with and without a short polyethlenglycol (PEG) spacer (9 atoms, -9.46 Å). In addition, different bpy-PNA sequences were prepared to leave a gap of 1– 4 unhybridized nucleobases between the hybridization sites of PNAs on the DNA template. The ligation reactions were performed at 40 °C, by irradiation of the mixture with blue light (455 nm, LED lamp, 1 W). Based on the difference in luminescence spectra between complexes **2** and **3**, we reasoned that we could follow the course of the reaction spectroscopically. Indeed, a clear bathochromic shift was observed after 1 h of reaction, with emission maxima shifting from 600 to 630 nm and exaltation of emission. Hence, the reactions were conveniently monitored by observing the increase of emission at 630 nm as a function of time (Figure 3A, B). Using this analysis, we compared the rates for the different ligation permutations (see Figure S1 in the Supporting Information for detailed kinetics). When comparing the size of the gap of unhybridized nucleobases for the series of reactions without PEG spacers, the reactions had comparable rates for a gap of 1–3 nucleobases, with a sharp decrease for a gap of 4 nucleobases. This suggests a cutoff point at which the size of the gap surpassed the distance between the linker and reagents required for an efficient reaction.

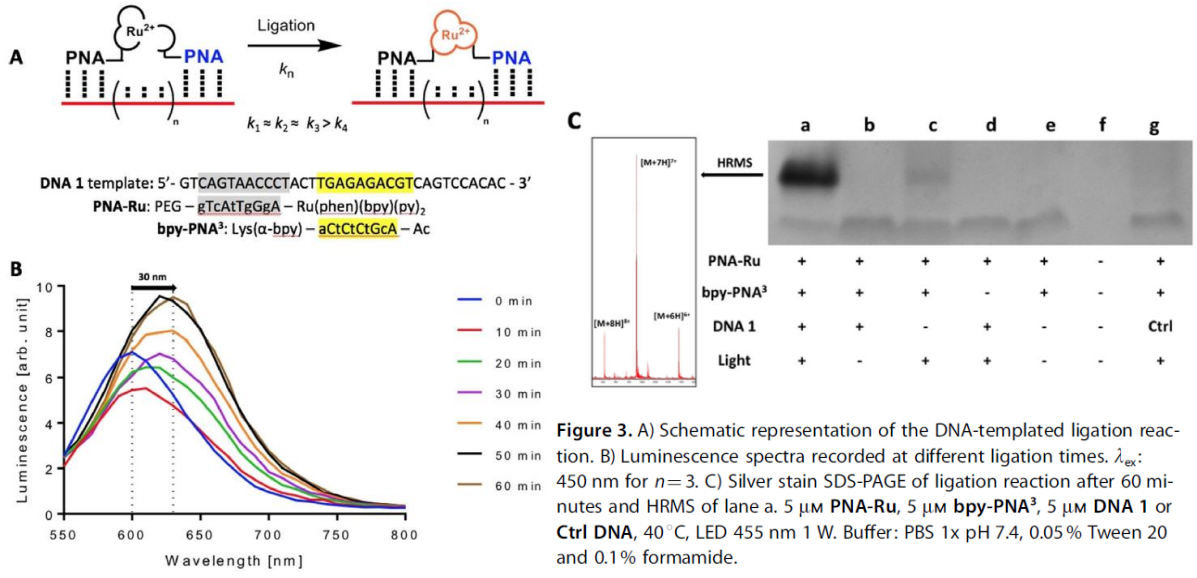

Figure 3. A) Schematic representation of the DNA-templated ligation reaction. B) Luminescence spectra recorded at different ligation times. λ_{ex}: 450 nm for $n = 3$. C) Silver stain SDS-PAGE of ligation reaction after 60 minutes and HRMS of lane a. 5 μM **PNA-Ru**, 5 μM **bpy-PNA**^{3}, 5 μM **DNA 1** or **Ctrl DNA**, 40 °C, LED 455 nm 1 W. Buffer: PBS 1x pH 7.4, 0.05% Tween 20 and 0.1% formamide.

The reactions with the PNAs bearing a PEG spacer were found to proceed slower than the corresponding reaction without PEGs, which is consistent with a reduced level of preorganization in the reactants. Based on these results, further reactions were carried out with probes lacking PEGs designed to leave a gap of three nucleobases between hybridization sites. It is interesting to note the decrease in luminescence (Figure 3B) at the very beginning of the reaction, which suggests an exchange between one of the two pyridine monodentate ligands of the ruthenium(II) complex with water as the first step prior to ligation.[32] Based on the titration curve of complex **3**, the yield of ligation was estimated to be >85 %. Performing the reaction in the absence of either template, light, or the PNA bearing the bipyridine ligand, failed to yield a bathochromic shift (Figure **S2**, Supporting Information), supporting that the observed ligation is a light-mediated and templated reaction. To unambiguously characterize the ligation product, the system was further analyzed by sodium dodecyl sulfate polyacrylamide gel electrophoresis (SDS-PAGE) of the crude reactions and HRMS (Figure 3 C). A bright stain for a higher molecular weight product was obtained only for the condition including the template and 450 nm light irradiation. HRMS analysis indeed showed the mass of the ligated product. Notably, the reaction had to be performed at relatively high concentration (5 mm; templated reaction with 10-mer PNAs are designed to operate at nm concentrations) to visualize the reagents and products on the gel. A marginal band corresponding to the product was also observed in lane c (Figure 3C) in the absence of template. The small amount of product observed under these conditions is attributed to unspecific hybridization of the **PNA-Ru** with **bpy-PNA** leading to product formation.

We next turned our attention to the use of the ligated product in catalytic reactions for nucleic acid sensing. To leverage the benefit of the high turnover potential of ruthenium photocatalysis, the reactions should be performed at high substrate concentrations. Thus, it is very important to have a reporter system with a very high turn-on ratio such that the product formed is not overshadowed by the large concentration of substrate. We had previously made use of a quinazolinone precipitating dye (QPD) with an azide-triggered immolation.[37] Contrary to other organic dyes, QPD is strongly fluorescent in the solid state and further benefits from a large Stokes shift and high photostability. The fluorescence in the solid state is given by an intramolecular proton transfer in the excited state (ESIPT). Considering that the phenolic hydrogen is essential for the fluorescence of QPD, the replacement with a caging group precludes any fluorescence. The turn-on performance of this system is thus far superior to regular caged fluorophore such as coumarin **4**. Based on the more recent discovery that pyridinium-based immolative linker provides a much faster uncaging than the azide-based immolative linker,[22] we prepared the new caged QPD **5** (Scheme 2). The pyridinium caging group was found to render the derivative highly soluble in water and non-fluorescent. These properties enable the use of high concentrations of substrate to maximize the rate of ruthenium(II)-photocatalyzed uncaging without compromising the signal with the background of a profluorophore. This new caged QPD complements the prior caged-QPDs that have been developed as probes for phosphatases,[38, 39] glycosidases,[40] peptidases.[41]

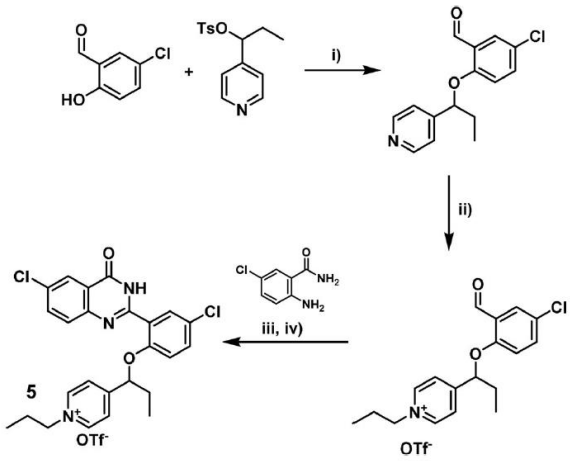

Scheme 2. Synthesis of caged QPD **5**. i) K_2CO_3, DMF, 60 °C, 6 h; ii) *n*PrOTf, DCM, −80 °C to RT, 1 h; iii) 1 equiv 2-amino-5-chlorobenzamide, TsOH, EtOH, reflux, 6 h; iv) DDQ, 0 °C to RT, 1 h.

The attractive properties of this dye (photostability, spatial contrast) have already inspired its use in nucleic acid imaging using an alkaline phosphatase conjugates in fluorescent in situ hybridization (FISH).[42–43] We reasoned that for soluble assays, confining the product of the templated reaction on a bead would localize the precipitate and enhance its detection. In our first design, streptavidin–agarose beads were loaded with a biotinylated version of **bpy-PNA³** (same sequence as shown in Figure 3) with a loading of 20 pmolmL1 of beads. The PNA containing ruthenium(II) precatalyst **2** (**PNA-Ru**, same sequence as shown in Figure 3) was added to the solution, and then matching DNA 1 was added at different concentrations. After a two-hour incubation, ligation was performed at 40°C using 455 nm LED irradiation. Beads were then placed under a microscope for visualization and the samples were irradiated with the laser of the microscope (argon laser, 488 nm) in the presence of profluorophore **5** and sodium ascorbate as the sacrificial reducing agent (Figure 4A).

Fluorescence of the precipitated QPD was assessed by twophoton(2P) excitation microscopy (730 nm 2P excitation, 500–550 nm emission). Although laser irradiation extended far outside the beads, we observed bright fluorescent precipitates only on the beads, and the precipitates were still detectable down to 0.01 equivalent of template (Figure 4B; see Figure S4 in the Supporting Information for the complete set of images). The quantification showed a direct correlation between the measured fluorescence values and the amounts of template used. The fluorescence of the beads without template or with 1 equivalent of non-complementary DNA was found to be significantly different from the lowest concentration tested (Figure 4 B). It should be noted that because the detection can be confined to a single bead of 70 µm, the detection of 0.01 equivalent of DNA analyte by the PNA capture probe represents a calculated detection threshold of 36 amol (amol=10^{-18} mol) of DNA per bead (estimate based on a bead loading of 20 pmolmL^{-1} and bead volume of 0.18 nL) and this detection threshold is independent of the volume used because it is confined to the bead. Considering that the formation of the precipitate is confined to the bead bearing the ligation product, we reasoned that beads of distinct size and/or shape could be derivatized with different PNA sequences to discriminate between multiple analytes, although the same detection reaction is used (QPD uncaging). To investigate the feasibility of this one-color multi-sequence detection, that is, to discriminate template sequences based on beads size, streptavidin agarose beads were filtered to separate beads with diameter bigger than 90 and smaller than 70 mm. The bigger beads were loaded with the biotinylated version of **bpy-PNA^{3}** previously used and small beads with a biotinylated version of a bpy-PNA conjugate that hybridizes to miRNA-21 (**bpy-PNA^{5}**, see Table S1 in the Supporting Information for sequence and explicit structure). Equal quantities of the beads were mixed and incubated alternatively with two different synthetic DNA templates in the presence of both the PNA-Ru targeting the different DNA sequences. Subsequent ligation and laser irradiation clearly showed the segregation of the precipitate depending upon the DNA sequence that was used. The non-complementary PNA-Ru probes also served as an internal negative control (Figure 5).

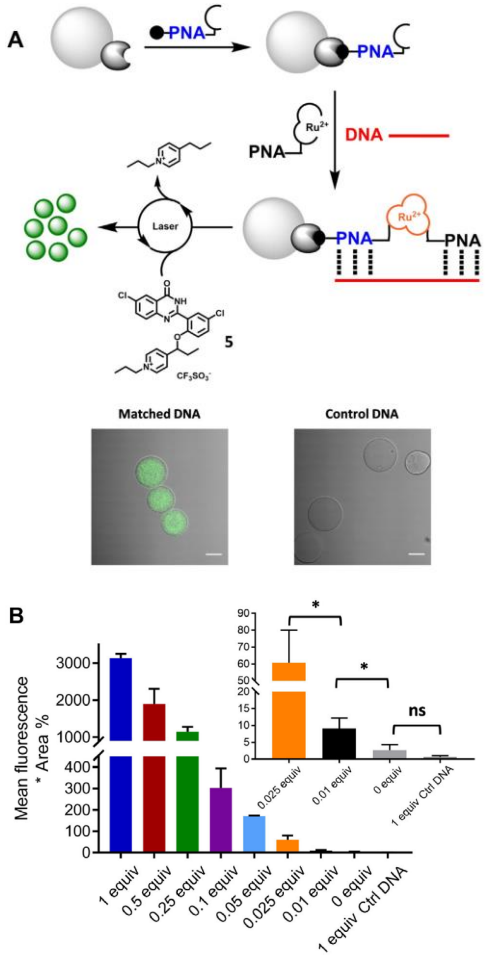

Figure 4. A) Scheme and representative images of QPD precipitation on beads. 100 nM **PNA-Ru**, 50 µM **5**, 10 mM sodium ascorbate, irradiation for 5 min with 488 nm laser, 100 % power. Buffer: PBS 1x pH 7.4, 0.05 % Tween 20 and 0.1 % formamide. λ_{ex}: 730 nm (2P excitation) 20 %, λ_{em}: 500–550 nm. Scale bar: 50 µm. Fluorescence is shown as a *Z*-maximum projection. B) Quantification of fluorescent precipitate on the beads at different template loading. $N=3$, two-tailed unpaired *t*-tests. * $p<0.05$, ns: non-significant.

We next investigated the possibility to apply the same chemistry to image cellular nucleic acids. Prior experiments showed that the use of a pyridinium-caged fluorophore is compatible with fixed cells conditions.[44] We chose to use MCF-7, a breast adenocarcinoma cell line that expresses moderately high level of miRNA-21, as a model.[45] Specifically, PFA-fixed cells were incubated with the corresponding PNA probes at 100 nm, 37°C for 2 hours. Ligation was performed at the same temperature, for 1 hour using 455 nm LED irradiation, then sodium ascorbate and caged QPD **5** were added and the cells further incubated for 1 hour. Following incubation, the cells were irradiated with 455 nm LED light for 30 minutes and the formation of fluorescent precipitates was visualized by microscopy. As shown in Figure 6, cells incubated with the PNAs designed to hybridize with miRNA-21 exhibited fluorescent precipitates localized in the cytosol, whereas no fluorescent precipitates were observed for the same experiment performed with non-complementary PNA sequences.

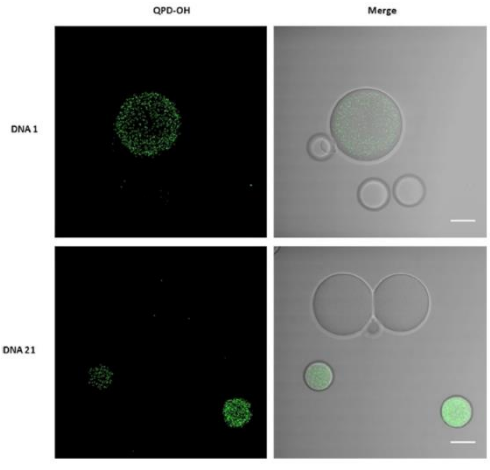

Figure 5. Representative images of DNA segregation on beads. 100 nM **PNA-Ru** and **PNA^{6}-Ru**, 100 nM **DNA 1** (top) or **DNA 21** (bottom), 50 µM **5**, 10 mM sodium ascorbate, irradiation for 1 min with laser line 488 nm, 100 % power. Buffer: PBS 1x pH 7.4, 0.05 % Tween 20 and 0.1 % formamide. λ_{ex}: 730 nm (2P excitation) 20 %, λ_{em}: 500–550 nm. Scale bar: 50 µm.

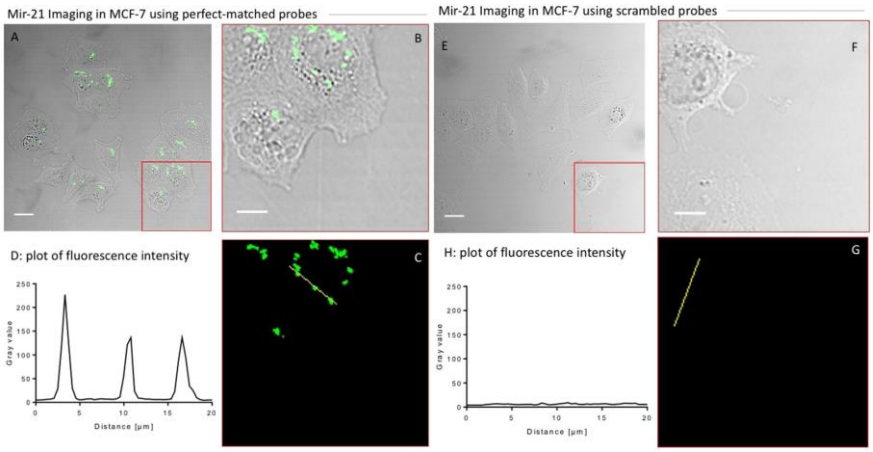

Figure 6. Representative images of templated ligation on fixed MCF-7 cells. Conditions: 100 nm **PNA^{6}-Ru**, 100 nm **bpy-PNA^{5}** or **bpy-PNA^{3}**, 20 µm 5, 20 mM sodium ascorbate, irradiation for 30 min with LED 455 nm 1 W. Buffer: DPBS (-). λ_{ex}: 730 nm (2P excitation) 20%, λ_{em}: 500–550 nm. Scale bar: 20 µm for A and E, 10 µm for B and F. A)–C) Reactions performed with the perfect match probes (**PNA^{6}-Ru** and **bpy-PNA^{5}**). E–F) Reaction performed with the scrambled probes (**PNA^{6}-Ru** and **bpy-PNA^{3}**). A,E) Overlay of differential interference contrast (DIC) with fluorescence images. B,F) Expanded views of the red quadrant in A and E, respectively. C,G) Fluorescence channel corresponding to B and F respectively, yellow lines denote the area that isquantified in quadrants E and H, respectively.

The afore-mentioned results make use of a catalyst formation that is conditional on the presence of a template (turn-on of catalysis). The reaction that yields the fluorescent readout is not templated and proceeds best at high substrate concentrations (>10 mm). We reasoned that our system could be extended to proceed at low substrate concentration, if an overhang sequence was adjacent to the catalyst for substrate hybridization. We had previously shown that a pentamer PNA was sufficient for PNA–PNA templated reactions.[22] This was achieved using a bifunctional bipyridine bearing a carboxylic acid group at the 5-position and a Fmoc-protected glycine conjugated to the 5'-amino group (Figure 7). The use of this bifunctional bipyridine allowed bpy-PNA synthesis to be continued to obtain a PNA-bpy-PNA adduct, using orthogonal Mtt/Fmoc chemistry.[36] To avoid crosstalk between the different stretches of this bifunctional PNA-bpy-PNA conjugate, the PNA hybridizing to DNA was prepared using chiral γ-L-PNA[22, 46], whereas the stretch hybridizing the substrate was prepared using chiral γ-D-PNA. For the detection, we made use of the caged coumarin because the reaction was performed in solution at low concentrations.

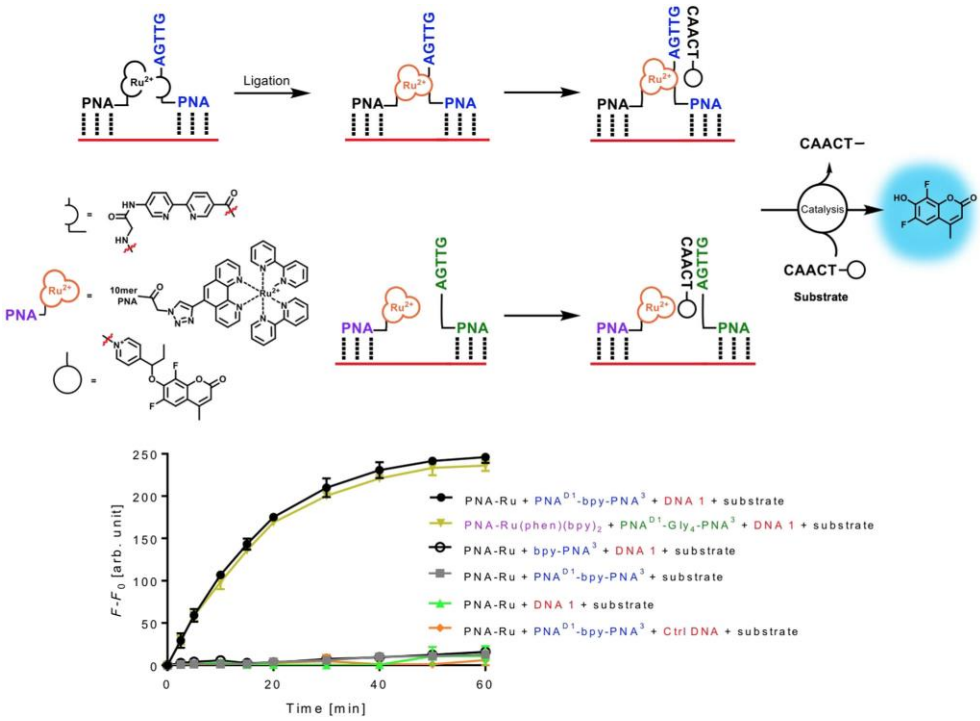

Figure 7. Templated release of a caged coumarin. 100 nM PNA probes and DNA, 10 mM sodium ascorbate, 40 °C, LED 455 nm 1 W. Buffer: PBS 1x pH 7.4, 0.05 % Tween 20 and 0.1 % formamide. λ_{ex}: 360 nm, λ_{em}: 460 nm.

The ligation was achieved as before, and the substrate was then added at a stoichiometric concentration (100 nm). Gratifyingly, the templated uncaging of coumarin proceeded well and reached completion after 60 min, whereas reaction performed under the same condition but without the template or with a non-

complementary DNA template afforded negligible conversion. When the reaction was performed under the same conditions but with bpy-PNA instead of PNA-bpy-PNA (i.e., a catalyst that cannot recruit the substrate), negligible reaction was observed, clearly highlighting the importance of substrate recruitment for reactions at low concentrations. We performed the same reaction under conditions that would not require template catalyst formation but would benefit from substrate recruitment. To this end, we used PNA-Ru(phen)$(bpy)_2$ instead of **PNA-Ru** (i.e., the PNA is conjugated to an active catalyst) and PNA-$(Gly)_4$-PNA instead of the PNA-bpy-PNA. The PNA-$(Gly)_4$-PNA cannot undergo ligation but can still recruit the substrate. Indeed, this reaction showed a complete conversion of the substrate. Notably, the kinetics of this latter reaction are very similar to those of the reaction performed with the ligation, suggesting that the ligation indeed delivered a fully functional catalyst.

CONCLUSION

In summary, we have described a new oligonucleotide-templated ligation for the synthesis of a photo catalytically active tris-heteroleptic Ru^{II} complex from catalytically inactive precursors. The ligation proceeded at physiological conditions, making use of light-promoted ligand exchange. The products of the ligations were used to uncage a QPD. Performing the reaction with probes that capture the ligation product on beads, we demonstrated a detection level of 36 amol of the DNA analyte per bead, suggesting that miniaturization of the assay to a single bead should afford attomole detection of analytes (DNA or RNA). This detection was multiplexed for multiple analytes with beads of distinct sizes. This technology was also applied to miRNA visualization in fixed cells. Finally, we demonstrated that this ligation also proceeds with a bifunctional bipyridine having one strand serving in the hybridization to the template (ligation chemistry, turn-on of photocatalysis) and a second strand for substrate recruitment (enabling the technology to operate at low substrate concentration).

ASSOCIATED CONTENT

Supporting Information

Supporting information and the ORCID identification number(s) for the author(s) of this article can be found under: https://doi.org/10.1002/chem.201804283.

ACKNOWLEDGMENT

The authors thank Marion Pupier for the NMR spectra of the ruthenium(II) complexes. UniGE bioimaging center provided the instruments for imaging. We thank the Swiss National Science Foundation for generous support (grant 200020 157106).

CONFLICT OF INTEREST

The authors declare no conflict of interest.

REFERENCES

[1] X. Li, D. R. Liu, *Angew. Chem. Int. Ed. Engl.* **2004**, *43*, 4848-4870.
[2] K. Gorska, N. Winssinger, *Angew. Chem. Int. Ed. Engl.* **2013**, *52*, 6820-6843.
[3] Y. Choi, G. Metcalf, M. H. Sleiman, D. Vair-Turnbull, S. Ladame, *Bioorg. Med. Chem.* **2014**, *22*, 4395-4398.
[4] M. Di Pisa, O. Seitz, *ChemMedChem* **2017**, *12*, 872-882.
[5] Y. Xu, N. B. Karalkar, E. T. Kool, *Nat. Biotechnol.* **2001**, *19*, 148-152.
[6] S. Sando, E. T. Kool, *J. Am. Chem. Soc.* **2002**, *124*, 2096-2097.
[7] H. Abe, E. T. Kool, *P. Natl. Acad. Sci. USA* **2006**, *103*, 263-268.
[8] Y. Huang, J. M. Coull, *J. Am. Chem. Soc.* **2008**, *130*, 3238.
[9] X. H. Chen, A. Roloff, O. Seitz, *Angew. Chem. Int. Ed. Engl.* **2012**, *51*, 4479-4483.
[10] Z. L. Pianowski, N. Winssinger, *Chem. Commun.* **2007**, 3820-3822.
[11] R. M. Franzini, E. T. Kool, *ChemBioChem* **2008**, *9*, 2981-2988.
[12] R. M. Franzini, E. T. Kool, *J. Am. Chem. Soc.* **2009**, *131*, 16021-16023.
[13] D. Al Sulaiman, J. Y. H. Chang, S. Ladame, *Angew. Chem. Int. Ed. Engl.* **2017**, *56*, 5247-5251.
[14] S. Ficht, C. Dose, O. Seitz, *ChemBioChem* **2005**, *6*, 2098-2103.
[15] O. Vazquez, O. Seitz, *J. Pept. Sci.* **2014**, *20*, 78-86.
[16] O. Zavoiura, U. Resch-Genger, O. Seitz, *Bioconjug. Chem.* **2018**, *29*, 1690-1702.
[17] J. Sayers, R. J. Payne, N. Winssinger, *Chem. Sci.* **2018**, *9*, 896-903.
[18] K. Fujimoto, S. Matsuda, N. Takahashi, I. Saito, *J. Am. Chem. Soc.* **2000**, *122*, 5646-5647.
[19] H. Wu, B. T. Cisneros, C. M. Cole, N. K. Devaraj, *J. Am. Chem. Soc.* **2014**, *136*, 17942-17945.

[20] H. Wu, S. C. Alexander, S. Jin, N. K. Devaraj, *J. Am. Chem. Soc.* **2016**, *138*, 11429-11432.
[21] K. K. Sadhu, N. Winssinger, *Chem. Eur. J.* **2013**, *19*, 8182-8189.
[22] D. Chang, E. Lindberg, N. Winssinger, *J. Am. Chem. Soc.* **2017**, *139*, 1444-1447.
[23] D. L. Chang, K. T. Kim, E. Lindberg, N. Winssinger, *Bioconjug. Chem.* **2018**, *29*, 158-163.
[24] J. L. Czlapinski, T. L. Sheppard, *J. Am. Chem. Soc.* **2001**, *123*, 8618-8619.
[25] D. K. Prusty, M. Kwak, J. Wildeman, A. Herrmann, *Angew. Chem. Int. Ed. Engl.* **2012**, *51*, 11894-11898.
[26] C. K. Prier, D. A. Rankic, D. W. MacMillan, *Chem. Rev.* **2013**, *113*, 5322-5363.
[27] F. Heinemann, J. Karges, G. Gasser, *Acc. Chem. Res.* **2017**, *50*, 2727-2736.
[28] L. Holtzer, I. Oleinich, M. Anzola, E. Lindberg, K. K. Sadhu, M. Gonzalez-Gaitan, N. Winssinger, *ACS Cent. Sci.* **2016**, *2*, 394-400.
[29] M. Roethlingshoefer, K. Gorska, N. Winssinger, *Org. Lett.* **2012**, *14*, 482-485.
[30] L. Zayat, M. Salierno, R. Etchenique, *Inorg. Chem.* **2006**, *45*, 1728-1731.
[31] L. Salassa, C. Garino, G. Salassa, R. Gobetto, C. Nervi, *J. Am. Chem. Soc.* **2008**, *130*, 9590-9597.
[32] J. C. Griepenburg, T. L. Rapp, P. J. Carroll, J. Eberwine, I. J. Dmochowski, *Chem. Sci.* **2015**, *6*, 2342-2346.
[33] J. Suffert, R. Ziessel, *Tet. Lett.* **1991**, *32*, 757-760.
[34] J. B. Borak, D. E. Falvey, *J. Org. Chem.* **2009**, *74*, 3894-3899.
[35] J. B. Edson, L. P. Spencer, J. M. Boncella, *Org. Lett.* **2011**, *13*, 6156-6159.
[36] D. Chouikhi, M. Ciobanu, C. Zambaldo, V. Duplan, S. Barluenga, N. Winssinger, *Chem. Eur. J.* **2012**, *18*, 12698-12704.
[37] K. K. Sadhu, E. Lindberg, N. Winssinger, *Chem. Commun.* **2015**, *51*, 16664-16666.
[38] Z. Huang, E. Terpetschnig, W. You, R. P. Haugland, *Anal. Biochem.* **1992**, *207*, 32-39.
[39] T. Machida, S. Dutt, N. Winssinger, *Angew. Chem. Int. Ed. Engl.* **2016**, *55*, 8595-8598.
[40] Z. L. Diwu, Y.; Upson, R. H.; Zhou, M.; Klaubert, D. H.; Haugland, R. P. , *Tetrahedron* **1997**, *53*, 7159-7164.
[41] M. Prost, L. Canaple, J. Samarut, J. Hasserodt, *ChemBioChem* **2014**, *15*, 1413-1417.
[42] V. B. Paragas, Y. Z. Zhang, R. P. Haugland, V. L. Singer, *J. Histochem. Cytochem.* **1997**, *45*, 345-357.
[43] J. Lu, A. Tsourkas, *Nucleic Acids Res.* **2009**, *37*, e100.
[44] J. Saarbach, E. Lindberg, S. Folliet, S. Georgeon, O. Hantschel, N. Winssinger, *Chem. Sci.* **2017**, *8*, 5119-5125.
[45] K. Ikeda, K. Horie-Inoue, T. Ueno, T. Suzuki, W. Sato, T. Shigekawa, A. Osaki, T. Saeki, E. Berezikov, H. Mano, S. Inoue, *Sci. Rep.* **2015**, *5*, 13170.
[46] I. Sacui, W. C. Hsieh, A. Manna, B. Sahu, D. H. Ly, *J. Am. Chem. Soc.* **2015**, 137, 8603-8610